IOP Publishing Measurement Science and Technology
Meas. Sci. Technol. **32** (2021) 045105 (12pp) https://doi.org/10.1088/1361-6501/abd1fd

Improved stochastic modeling of multi-GNSS single point positioning with additional BDS-3 observations

Hong Hu[1,3], **Feng Zhou**[2] **and Shuanggen Jin**[4,5,6]

[1] School of Resources and Environmental Engineering, Anhui University, Hefei 230601, People's Republic of China
[2] College of Geomatics, Shandong University of Science and Technology, Qingdao 266590, People's Republic of China
[3] Anhui Province Key Laboratory of Wetland Ecosystem Protection and Restoration, Anhui University, Hefei 230601, People's Republic of China
[4] School of Remote Sensing and Geomatics Engineering, Nanjing University of Information Science and Technology, Nanjing 210044, People's Republic of China
[5] Shanghai Astronomical Observatory, Chinese Academy of Science, Shanghai 200030, People's Republic of China
[6] Jiangsu Engineering Center for Collaborative Navigation/Positioning and Smart Applications, Nanjing University of Information Science and Technology, Nanjing 210044, People's Republic of China

E-mail: huhong@ahu.edu.cn and sgjin@shao.ac.cn

Received 30 August 2020, revised 26 November 2020
Accepted for publication 9 December 2020
Published 17 February 2021

Abstract

The accuracy of Global Navigation Satellite System (GNSS) observations is affected by many factors, such as different systems, frequencies, carriers and pseudoranges, all of which also vary with different situations. Therefore, it is challenging to establish an accurate stochastic model for multi-GNSS positioning in theory, particularly for the additional BeiDou-3 Global Navigation Satellite System (BDS-3). In practical applications, the real stochastic model needs to be estimated based on the characteristics of the observations themselves. We evaluated the influence of BDS-3 on the positioning results using 46 sites distributed around the world and proposed an improved stochastic model for multi-GNSS single point positioning (SPP) based on the least-squares variance component estimation (LS-VCE). The results show that when the BDS-3 observations are added, the positioning precision and accuracy are significantly improved. By using the improved LS-VCE method in GPS/BDS dual system positioning, the accuracy of E, N and U directions are 0.373, 0.498 and 1.044 m, respectively, when compared to the traditional method with 0.502, 0.533 and 1.333 m. The proposed stochastic model improves the multi-GNSS SPP accuracy without significantly increasing the calculation time. Furthermore, reliable results are obtained for all epochs with the improved LS-VCE model.

Keywords: BDS-3, stochastic model, LS-VCE, multi-GNSS, single point positioning

(Some figures may appear in colour only in the online journal)

1. Introduction

Generally, a complete Global Navigation Satellite System (GNSS) observation model consists of functional and stochastic models. Establishing more accurate functional and stochastic models is the premise for obtaining optimal solutions during GNSS data processing [1]. The functional model describes the functional relationship between the observations and estimated parameters, while the stochastic model reflects the statistical characteristics of the observations, including observation precision and their correlations among each other and in time. The stochastic model can actually be

Table 1. BDS open service signals and the corresponding satellites.

Signal frequency	Satellites	Services
B1I	3 IGSO + 24 MEO + 3 GEO	Basic navigation services (global/ regional)
B1C	3 IGSO + 24 MEO	
B2a	3 IGSO + 24 MEO	
B3I	3 IGSO + 24 MEO + 3 GEO	
B2b	3 GEO	Precise Point Positioning service (regional)

expressed by a covariance matrix, being the second-order central moments of the elements of the random observation errors. Only when the correct stochastic model is employed one can obtain minimum variance estimators of the estimated parameters in a linearized GNSS functional model [2, 3]. Moreover, rigorous GNSS data processing also requires reliable statistical tests depending on the covariance matrix, while such statistical tests are known to be sensitive to the stochastic model [4–6].

Earlier studies of the GNSS stochastic model were primarily based on the elevation dependence of random observation errors [7, 8]. Due to its simplicity and high computational efficiency, most existing GNSS software packages implement methods based on the elevation dependence of observation variances, i.e. BERNESE, GAMIT, and RTKLIB [9–11]. Later, the stochastic model started to take time and cross correlations among observations into account by using variance component estimation (VCE) and least-squares variance component estimation (LS-VCE) methods [12–14]. Furthermore, the signal-to-noise-ratio based models, i.e. SIGMA-ε and SIGMA-δ [15–18]. However, these stochastic models are mainly for GPS signals and observations. To account for the differences between the stochastic properties of GPS and BeiDou Global Navigation Satellite System (BDS-2) observations owing to the differences in their constellations and signal quality, Li *et al* [19, 20] demonstrated a systematic study of the estimation, assessment, and impact of the BDS-2 stochastic model on positioning performance.

The new-generation BeiDou-3 Global Navigation Satellite System (BDS-3) project started in 2009, and the first new-generation BDS-3 satellite was launched on 5 November 2017. At present, 30 BDS-3 constellation satellites (including 24 medium Earth orbit (MEO) satellites, three geostationary Earth orbit (GEO) satellites and three inclined geosynchronous orbit (IGSO) satellites) have been successfully launched, and stable and reliable inter-satellite links have been established. For the new-generation BDS-3 satellites, new signals, satellite attitude modes, and atomic clocks have been applied. The experimental BDS-3 satellites transmit signals on five frequencies, including backward-compatible B1I (1561.098 MHz) and B3I (1268.52 MHz), and new B1C (1575.42 MHz), B2a (1176.45 MHz) and B2b (1207.14 MHz) [21, 22]. BDS provides open service through various types of satellites in 2020 are given in table 1 [23].

Numerous studies have focused on BDS-3 precise satellite orbit and clock determination [22], precise point positioning (PPP) [24, 25], single point positioning (SPP) [26] and GPS/BDS dual system positioning [27, 28]. However, very few studies have involved the stochastic model for BDS-3 observations [29, 30]. Actually, BDS-3 has shown a more diverse signal structure, which will certainly bring more challenges to stochastic modeling. The differences in stochastic models for BDS-3, BDS-2, and GPS should be clearly indicated, and the stochastic model for BDS-3 signals and observations needs to be studied and investigated further.

Considering the complexity of the stochastic model and its dependence on receiver type, the antenna type and observation environment, in practical applications, one should estimate the realistic stochastic model with the data set itself [20]. We used 46 globally distributed stations to evaluate the contribution of BDS-3 to the positioning and proposed an improved stochastic model based on LS-VCE. The organization of this work proceeds as follows. We start with a brief representation of an SPP mathematic model including a functional model and a stochastic model, the description of LS-VCE, and the implementation of LS-VCE in multi-GNSS SPP processing. Afterward, the performance of different stochastic models including our improved model on SPP accuracy is demonstrated and compared. Finally, we end with a summary and conclusions.

2. SPP observation models for combined GPS and BDS

In this section, we will describe the functional model and the stochastic model for combined GPS and BDS observations, followed by the description of the LS-VCE method. The section ends with the application of LS-VCE to multiple GNSS.

2.1. Functional model and stochastic model

The combined GPS and BDS functional model is based on a non-linearized equation and can be expressed by the following equations:

$$\begin{aligned} P_{\mathrm{G},r}^{s}(t_i) &= \rho_{0\,r,\mathrm{G}}^{s}(t_i) + c(\mathrm{d}t_{\mathrm{G},r}(t_i) - \mathrm{d}t_{\mathrm{G}}^{S}(t_i)) + T_{r,\mathrm{G}}^{s}(t_i) \\ &\quad + I_{r,\mathrm{G}}^{s}(t_i) + \varepsilon_{P_{\mathrm{G}}r}^{\ s}(t_i) \\ P_{\mathrm{C},r}^{s}(t_i) &= \rho_{0\,r,\mathrm{C}}^{s}(t_i) + c(\mathrm{d}t_{\mathrm{C},r}(t_i) - \mathrm{d}t_{\mathrm{C}}^{S}(t_i)) + T_{r,\mathrm{C}}^{s}(t_i) \\ &\quad + I_{r,\mathrm{C}}^{s}(t_i) + \varepsilon_{P_{\mathrm{C}}r}^{\ s}(t_i) \end{aligned} \tag{1}$$

where the superscript s and subscript r indicate the satellite and receiver number, respectively, c is the speed of light in vacuum, P_G and P_C are the code observation of GPS and BDS, $\mathrm{d}t_{G,r}$ and $\mathrm{d}t_{C,r}$ are the receiver clock error of GPS and BDS, respectively. ρ_0 is the geometric distance between receiver at reception time and satellite at transmission time, $\mathrm{d}t^s$ is the satellite clock error, T is the tropospheric delay, I is the first-order ionospheric delay, the subscripts G and C denote GPS and BDS, respectively. Ionospheric and tropospheric errors are corrected by using the Klobuchar model [31] and the Saastamoinen model [32], respectively. t_i indicates the time instant or epoch to which the observations refer, and ε is the

pseudorange measurement noise contains the multipath error, ephemeris error and the residual errors of ionospheric and tropospheric, etc.

In many practical applications, the covariance is only partly known. For a single epoch dual system SPP, the linearized model of observation equations can be written as [33, 34]

$$\begin{aligned} dL &= A \cdot dx + e \\ Q_L &= Q_0 + \sum_{k=1}^{p} \sigma_k Q_{Lk} \end{aligned} \tag{2}$$

where dL is the vector of observables, m is the number of satellites tracked, $\boldsymbol{e}$ is a measurement error vector, $\boldsymbol{dx}$ is the $n \times 1$ correction vector of unknown parameters, $\boldsymbol{A}$ is the $m \times n$ design coefficient matrix, Q_L is the covariance matrix of the observables, and Q_0 is the known part of the variance matrix. In most cases, Q_0 is a null matrix. The cofactor matrix Q_{Lk} is assumed to be known. The unknown variance-covariance components σ_k ($k = 1, \ldots, p$) are to be estimated using VCE. p is the number of total types of observations after classification.

The estimated positioning results using least-squares can be expressed as

$$\begin{aligned} \boldsymbol{dx} &= (\mathbf{A}^T \mathbf{Q}_L^{-1} \mathbf{A})^{-1} \mathbf{A}^T Q_L^{-1} dL \\ \hat{X} &= \mathbf{X}_0 + \boldsymbol{dx} \\ Q_{XX} &= (A^T Q_L^{-1} A)^{-1} \end{aligned} \tag{3}$$

$$Q_{XX} = (A^T Q_L^{-1} A)^{-1} = \begin{bmatrix} q_{11} & q_{12} & q_{13} & q_{14} & q_{15} \\ q_{21} & q_{22} & q_{23} & q_{24} & q_{25} \\ q_{31} & q_{32} & q_{33} & q_{34} & q_{35} \\ q_{41} & q_{42} & q_{43} & q_{44} & q_{45} \\ q_{51} & q_{52} & q_{53} & q_{54} & q_{55} \end{bmatrix} \tag{4}$$

where X_0, Q_{XX} are the initial value and covariance matrix of the unknown parameters, respectively, q_{ij} ($i, j = 1,2,\ldots5$) is the element in the covariance matrix. Then the precision of the estimated position in local coordinate system can be written as

$$Q_{ENU} = R Q_{XYZ} R^T \tag{5}$$

where $Q_{XYZ} = \begin{bmatrix} q_{11} & q_{12} & q_{13} \\ q_{21} & q_{22} & q_{23} \\ q_{31} & q_{32} & q_{33} \end{bmatrix}$ is the coordinate part of the covariance, R is the rotation matrix from geodetic coordinate system to local coordinate system.

2.2. LS-VCE

There are many different VCE methods such as Helmert VCE [35], the best invariant quadratic unbiased estimator [2, 36], the minimum norm quadratic unbiased estimator [37], the restricted maximum likelihood estimator [38], and LS-VCE [33, 39, 40]. These methods might be equivalent under certain conditions [13, 19, 33, 41]. LS-VCE gives the unknown variance-covariance components by

$$\hat{\sigma} = N^{-1} l \tag{6}$$

where $\hat{\sigma} = [\hat{\sigma}_1, \ldots, \hat{\sigma}_p]^T$, the $p \times p$ matrix $\boldsymbol{N}$ and p column vector $\boldsymbol{l}$ are obtained as [33]

$$n_{ij} = \frac{1}{2} tr(Q_{Li} Q_L^{-1} P_A^{\perp} Q_{Lj} Q_L^{-1} P_A^{\perp}) \tag{7}$$

$$l_i = \frac{1}{2} \hat{e}^T Q_L^{-1} Q_{Li} Q_L^{-1} \hat{e} - \frac{1}{2} tr(Q_0 Q_L^{-1} P_A^{\perp} Q_{Li} Q_L^{-1} P_A^{\perp}) \tag{8}$$

where tr is the trace operator that computes the summation of all diagonal elements of a matrix, Q_{Li} and Q_{Lj} ($i, j = 1,2,\ldots p$) represent the variance matrix of different types of observations, respectively, $\hat{e} = P_A^{\perp} L$ is the least-squares residuals, the $m \times m$ matrix $P_A^{\perp} = I - A(A^T Q_L^{-1} A)^{-1} A^T Q_L^{-1}$ is the orthogonal projection of $\boldsymbol{A}$, and the covariance matrix of the variance components is $Q_{\hat{\sigma}} = N^{-1}$. Because $Q_0 = \mathbf{0}$, equation (8) can be rewritten as

$$l_i = \frac{1}{2} \hat{e}^T Q_L^{-1} Q_{Li} Q_L^{-1} \hat{e}. \tag{9}$$

In LS-VCE, one estimates the unknown variance-covariance component in an iterative manner because the covariance matrix Q_L and the orthogonal projection $P_A^{\perp}$ are functions of the unknown variance components. The cofactor matrix is given according to the empirical precision of the observations [42, 43]. The elevation-dependent model (EDM) was adopted for the initial Q_{Lk} because it is widely used [19]. The iteration continues until the convergence value is obtained, which means that the difference in the computed unknowns between two consecutive iterations must be less than the tolerance ε:

$$\left\| \hat{\sigma}^j - \hat{\sigma}^{j-1} \right\| < \varepsilon \tag{10}$$

where $\|\bullet\|$ denote a vector norm and $\varepsilon = 10^{-6}$.

2.3. Implementation of LS-VCE in multi-GNSS SPP

The variance component is very important for multi-GNSS precise positioning, especially in cases where the precision of some types of observations is unknown. As an example, we simply divide the observations into two types: GPS and BDS. The observation equations of multi-GNSS SPP reads

$$E\begin{pmatrix} P_G(t_i) \\ P_C(t_i) \end{pmatrix} = Ax \tag{11}$$

where $P_G(t_i)$ and $P_C(t_i)$ denote the pseudorange observations of GPS and BDS at the measurement time instant t_i. $\boldsymbol{x} = \begin{bmatrix} X & Y & Z & c \cdot dt_{G,r} & c \cdot dt_{C,r} \end{bmatrix}^T$ are the unknown parameters. The design coefficient matrix $\boldsymbol{A}$ is partitioned as

$$A = [A_1 A_2] \text{ with } A_1 = \begin{bmatrix} \Lambda_G \\ {\scriptstyle m \times 3} \\ \Lambda_C \\ {\scriptstyle n \times 3} \end{bmatrix} \text{ and } A_2 = \begin{bmatrix} 1 & 0 \\ {\scriptstyle m \times 1} & \\ 0 & 1 \\ & {\scriptstyle n \times 1} \end{bmatrix} \tag{12}$$

where m and n are the number of GPS and BDS tracked satellites, respectively. Λ is the unit direction vector between satellite and receiver (for example, receiver r to satellite j), the unit direction vector is $\Lambda_r^j = -(r^j - r_r) / \left\| r^j - r_r \right\|$, with the vector

Table 2. The receiver types of receivers and their corresponding numbers utilized in the experiment.

Manufacturer	Type	Number
TRIMBLE	NETR9	13
LEICA	GR10	1
	GR25	3
Septentrio	POLARX4	7
	POLARX4TR	2
	POLARX5	9
	POLARX5TR	5
JAVAD	TRE_3	3
	TRE_3 DELTA	3

r^j and r_r as the geocentric vectors of satellite j and receiver r, respectively. The observations are assumed to be independent in standard point positioning, so the cross-correlations are set to zeros. The time correlation is also ignored because of single epoch SPP is applied. Then the single epoch stochastic model reads

$$Q_L = \sigma_G \begin{bmatrix} Q_G & 0 \\ 0 & 0 \end{bmatrix} + \sigma_C \begin{bmatrix} 0 & 0 \\ 0 & Q_C \end{bmatrix} \tag{13}$$

where σ_G and σ_C are variance components of GPS and BDS, and the initial value of the variance components are all 1. Q_G and Q_C are diagonal matrices, and the initial values of the diagonal elements of the two matrices are given by the EDM. In that case, the following three-step estimation procedure is proposed for multi-GNSS SPP. The first step is to determine the number of types of observables based on their characteristics and give values of the initial variance matrix according to the EDM. The second step is to estimate the variance component using LS-VCE. The third step is to update the variance-covariance matrix and calculate the parameters to be estimated using least squares.

3. Estimation of the multi-GNSS stochastic model

To ensure the reliability of the results, we use 46 globally distributed stations, as shown in figure 1. The receivers deployed in these 46 stations are from four GNSS receiver manufacturers, and nine types are involved. Table 2 presents the types and their numbers employed in the experiment. Three of the stations cannot track signals from BDS-3 satellites, and these stations are marked with triangles in figure 1.

All observation datasets were collected by the Multi-GNSS Experiment (MGEX), which is being operated by the International GNSS Service (IGS). Some of these stations only have the capacity of tracking BDS-2 signals, because the Space Interface Control Document was not finally released until August 2020. Moreover, observations from some BDS-3 satellites may be wrong because the receivers do not work properly for BDS-3. Without loss of generality, the single-frequency SPP was performed with pseudorange observations from GPS L1 and BDS B1 frequencies. BDS-3 adopts the BeiDou Coordinate System (BDCS). The definition of BDCS is in accordance with the specifications of the International Earth Rotation and Reference System Service, and it is consistent with the definition of the China Geodetic Coordinate System 2000 (CGCS2000) [44], which is adopted by BDS-2. The difference between the coordinate systems is negligible for pseudorange-based SPP because the difference between CGCS2000 and WGS84 is at the level of a few centimeters [34].

Only 18 BDS-3 satellites have been operating as of 1 May 2019. This does not mean that all worldwide users can determine their locations using BDS-3. There are fewer than four BDS-3 satellites tracked in some regions, particularly those in the Western Hemisphere. Therefore, we first arbitrarily estimate the variance components of BDS-2 and BDS-3 as a type of observations and evaluate the impact on the precision of standard point positioning with the addition of BDS-3 observations. Second, an Asian station, with more BDS-2 and BDS-3 satellites tracked, is chosen for analyzing the impact of different stochastic models on positioning accuracy. Finally, an optimized stochastic model will be given and the performance and reliability of the new model will be verified using the 46 sites distributed globally.

3.1. Positioning accuracy and precision improvement with the additional BDS-3 observations

SPP is widely used in the positioning and navigation of various dynamic carriers; as a result, we first estimate the coordinates and evaluate the accuracy epoch by epoch. As already discussed by Hu *et al* [42], the GPS C/A code and BDS B1 code observations exhibit a strong relationship with their elevations, with the precision of observations improving as the elevation angle increases. Moreover, the most popular stochastic model is based on EDM. Therefore, we calculate the coordinate accuracy of 46 stations using the GPS system and the GPS-BDS dual system, in which the EDM is adopted as a comparison. The reference coordinates of these 46 sites are also provided by IGS. We estimated the SPP solutions at every epoch using least squares and calculated the root mean square (RMS) values of the coordinate residuals. However, in practical applications, we cannot obtain the reference coordinates to calculate the RMS values. The covariance matrix is usually used to indicate the quality of the positioning results. Hence, the precision by taking the average over all epochs that come from the covariance matrix in a single day is also employed to evaluate the quality of the positioning results. Subsequently, we can obtain the average RMS and precision values for 46 stations. The statistical results of the average RMS of the residuals listed in table 3 provide the evidence that the positioning accuracy of the dual system has not improved significantly. Comparing the accuracy improvement in the east (E), north (N), and up (U) components, we find that 31 sites have improved E-component accuracy, 38 sites have improved N-component accuracy, and 35 sites have improved U-component accuracy. However, with the addition of BDS observations, some sites exhibit poorer accuracy, whereas the accuracy in all three directions is significantly

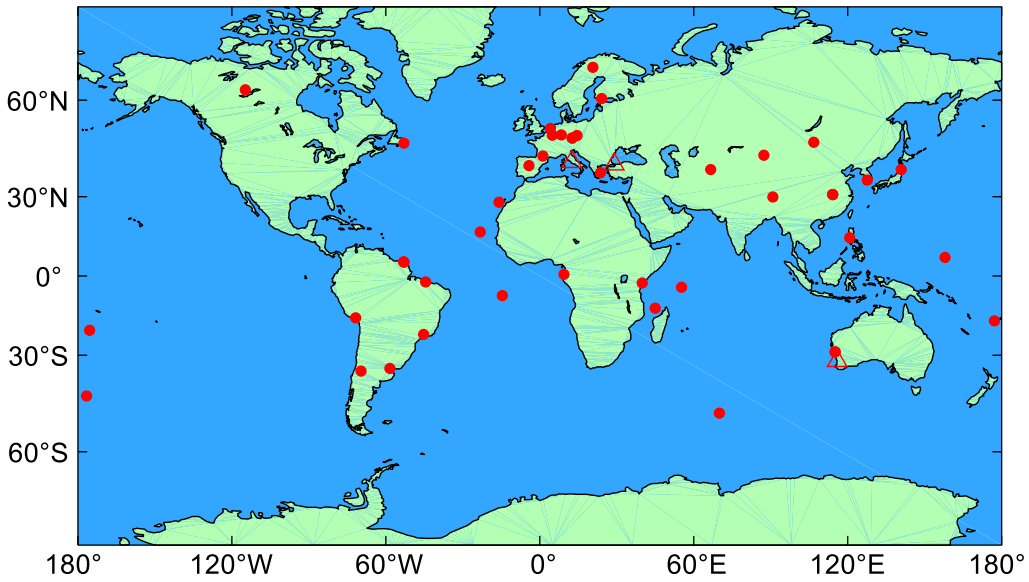

Figure 1. Distribution of the sites used in the experiment. The selected 46 IGS-MGEX station datasets are over the entire 24 h of day of the year (DOY) 96 in 2019. Three of these sites can only provide BDS-2 observations; these stations are represented by open triangles in the map, and other sites are represented by solid circles.

Table 3. Average RMS values using different stochastic models (in meters).

Component	GPS only	GPS and BDS	GPS/BDS LS-VCE
E	0.4877	0.5018	0.3786
N	0.6358	0.5333	0.4977
U	1.3685	1.3334	1.0652

improved by using the LS-VCE method in dual system positioning.

Figure 2 shows the relationship between the percentage improvements in accuracy and the number of sites compared to that of the single GPS system. The traditional EDM exhibits positioning accuracy improvement in most of the 46 stations. However, for some sites, the positioning accuracy deteriorates, which may be because of the fewer BDS satellites in some areas. In addition, when we analyzed the receiver models of these sites, we found that these receivers are basically from the same manufacturer. As shown in figure 2, when LS-VCE is used to recalculate the positioning accuracy of the dual system observations, no site accuracy exceeds −20%, and the accuracy of all sites is improved or nearly at the same level.

Taking two stations WUH2 and YEL2 in each of the eastern and western hemispheres as examples to analyze the precision obtained by different methods. Figure 3 shows the precision sequence of each epoch using GPS only, GPS/BDS dual system EDM and LS-VCE. By comparing the results, we found that using dual systems can significantly improve the precision in each direction. The average precision in E, N and U direction obtained by LS-VCE is better than that of EDM. However, the LS-VCE method is affected by matrix inversion and the number of loops during the data processing, and

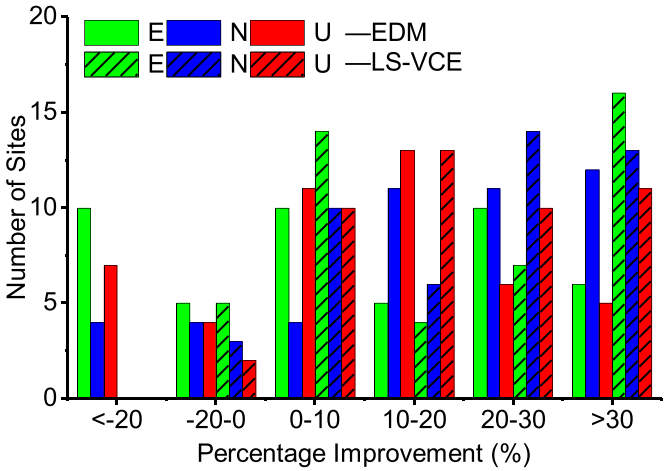

Figure 2. Number of sites influenced by the addition of BDS observations. The three solid color histograms represent the improvement in accuracy with respect to a single GPS system in the three directions E, N, and U, and the slashed columns represent the accuracy improvement in the three directions after LS-VCE.

its precision envelope is not as smooth as that of EDM. The statistical results of the precision using different methods are shown in figure 4.

Figure 4 depicts the boxplot of the precision of the 46 sites in the E, N, and U directions using EDM and LS-VCE methods compared to that of the single GPS system. As shown in the figure, the overall precision of the three directions using dual system is significantly improved compared to that of the single GPS system. The median precision is 0.706, 0.529 and 0.350 m in the E direction, 0.876, 0.604 and 0.378 m in the N direction, and 1.817, 1.312 and 0.828 m in the U direction using GPS only, EMD and LS-VCE, respectively. However,

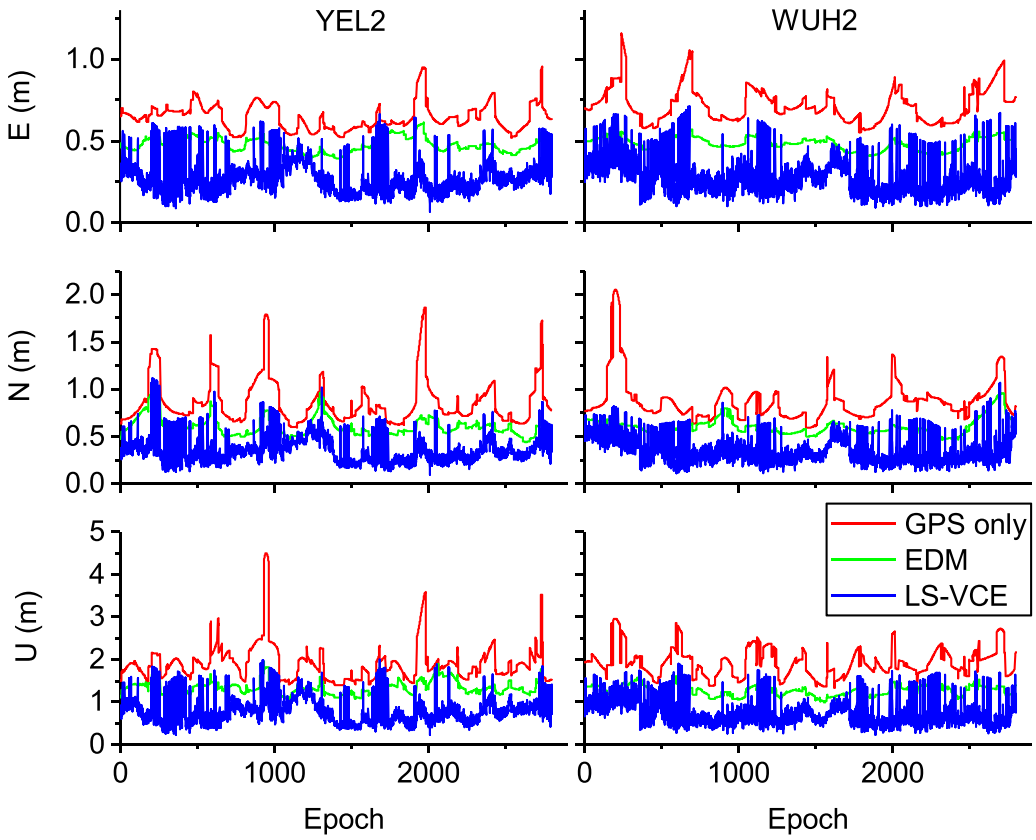

Figure 3. Precision sequence of YEL2 and WUH2 derived from GPS only, EDM and LS-VCE. The red line, green line and blue line represent the results sequence of E, N and U components obtained by GPS only, EDM and LS-VCE respectively.

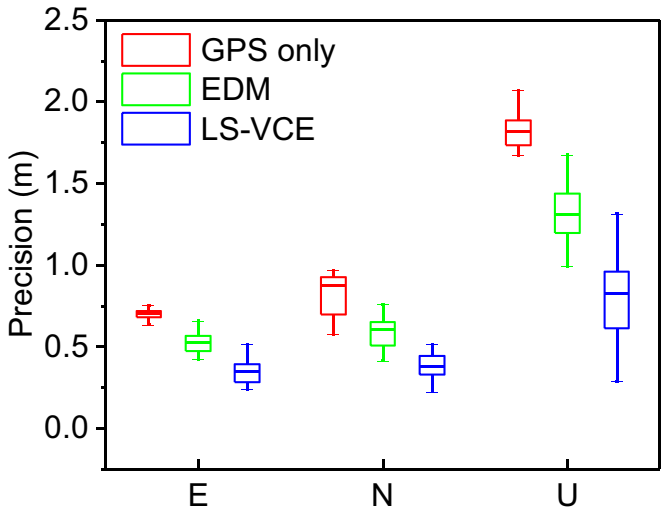

Figure 4. Boxplot of E, N and U direction precision derived from EMD and LS-VCE model compared with GPS only.

when the number of BDS satellites is significantly less than that of GPS, the covariance matrix obtained by the LS-VCE method will fail to converge, which will lead to reduced positioning precision.

Therefore, we can speculate that, if we do not choose the correct stochastic model, the addition of BDS observations does not necessarily improve positioning accuracy. However, it should be pointed out that the LS-VCE method encounters a case in which about 5% of the total epochs could have negative values in the variance-covariance matrices in some epochs and the residuals could be much larger than those in other epochs. In the results of table 3, we simply omitted these epochs directly, so the statistics are not comprehensive.

Figure 5 shows the number of visible satellites all over the world with the elevation cut off angle of 10° at UTC time 4:00 on DOY 47, 2019. Figure 5 shows that 4–14 satellites can be tracked worldwide with GPS only, while, with BD2 only, the minimum number of satellites that can be tracked in the Western Hemisphere is zero. The subfigure labeled GPS/BDS-2 shows the number of visible satellites under the GPS, BDS-2 dual system. The maximum number of satellites is 27 and the minimum number is 5. The subfigure labeled GPS/BDS-2 + 3 shows the number of visible satellites under GPS, BDS-2, and BDS-3. The maximum number of visible satellites is 32 and the minimum number is 6. The use of BDS-3 can increase the number of visible satellites, and the observations are more redundant, which is especially important for estimating the unknown parameters.

3.2. Data analysis in a single site with the additional BDS-3 observations

The station WHU2, which is located in China in the mid-latitudes of the Northern Hemisphere, is chosen to meet the purpose of obtaining more BDS observations to evaluate the

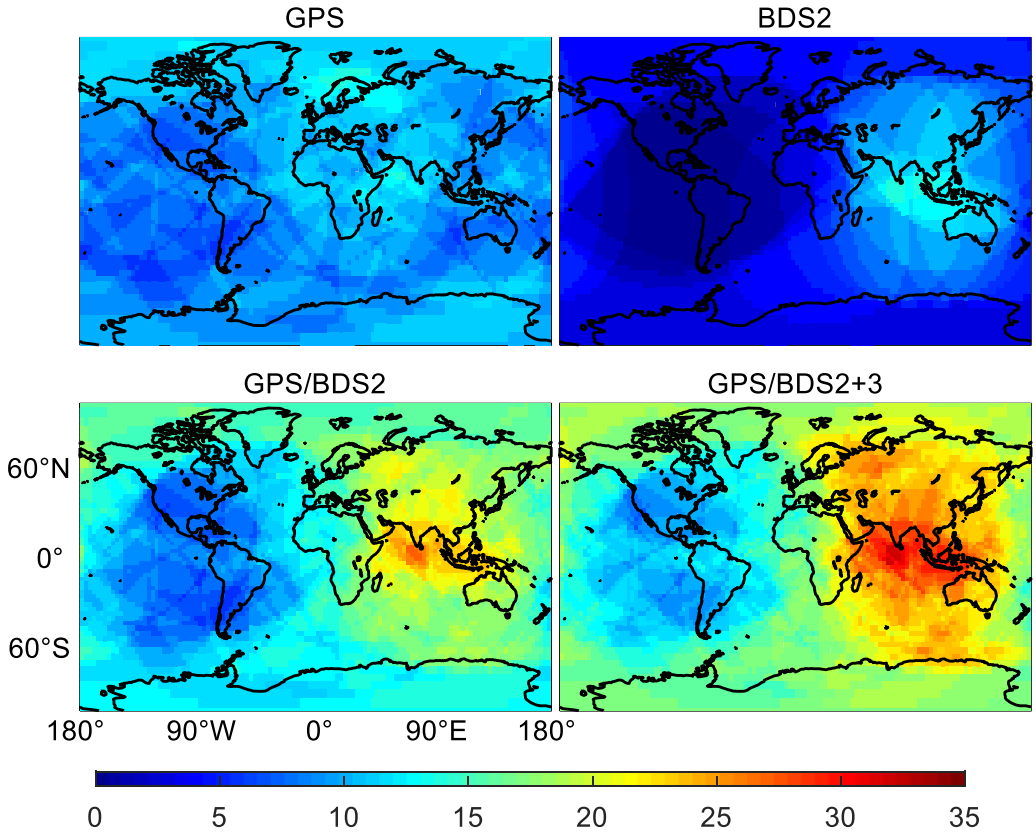

Figure 5. Number of satellites visible at the same time over the world (top) under GPS only and BDS-2 only, respectively, (bottom left) under the GPS–BDS-2 dual system, and (bottom right) under GPS, BDS-2, and BDS-3.

impact of BDS on the positioning results. Figure 6 indicates that more BDS-2 satellites can be tracked most of the time, compared with GPS satellites at this site. In contrast, the number of BDS-3 satellites is generally less than that of BDS-2 and GPS, with sometimes only two satellites capable of being tracked. In other words, using BDS-3 only does not guarantee that positioning can be done anywhere at any time. Therefore, the position dilution of precision (PDOP) for BDS-3 alone is not shown in figure 7. The PDOP is a factor, which indicates the factor of precision of the position [45], and the PDOP values can be computed based on the diagonal elements of the cofactor matrix of the receiver position [34]. For WHU2, during most of the day, the average PDOP values of BDS-2 or GPS only are basically equal, and the PDOP value of BDS-2 does not appear to be greater than 3.5. When adding BDS-3 satellites, the value of BDS PDOP becomes significantly smaller than that of GPS. Moreover, when we merged the two systems for positioning, the value of PDOP was significantly reduced. Therefore, as can be seen from figures 4 and 5, the use of BDS-3 cannot only increase the number of visible satellites but also enhance the spatial geometric strength of the satellites to reduce the PDOP value.

The residuals calculated by GPS only, BDS-2, and BDS-2 + BDS-3 based on the EMD with an elevation cut off angle of 10° are shown in figure 8. It can be seen from the figure that the east direction (E) component has the best accuracy and the up direction (U) component has the poorest. The RMS

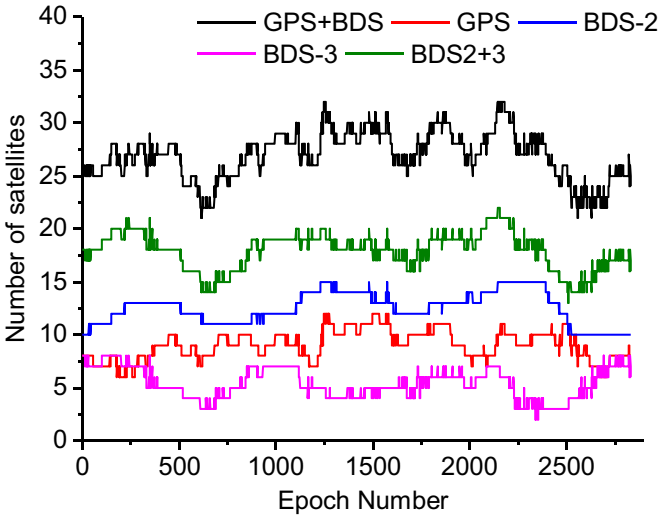

Figure 6. Number of tracking satellites from different constellations over 24 h at the WHU2 station.

values for E, N, and U components for GPS only SPP are 0.326, 0.737 and 1.249 m, respectively. The RMS values for BDS-2 SPP are 0.464, 0.562 and 1.292 m, respectively. The precision in the three directions of E, N and U is 0.717, 0.872 and 1.917 m for GPS only, and 0.692, 1.030 and 1.958 m for BDS-2. Because only two or three satellites can be observed, we do not compare the precision and RMS values using BDS-3

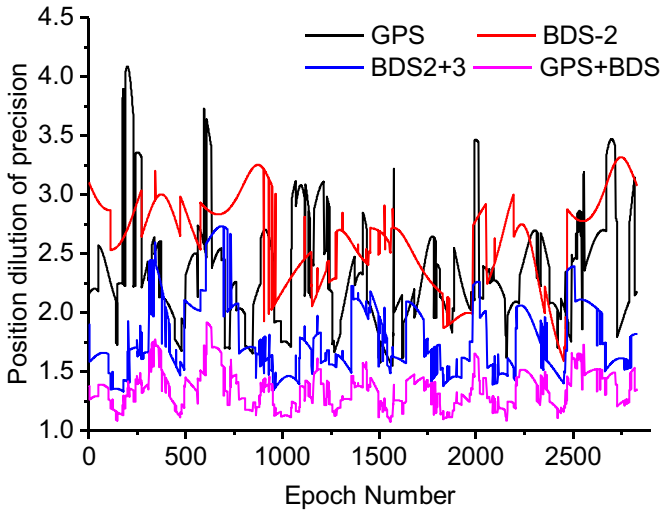

Figure 7. PDOP of satellites for GPS only, BDS-2 only, BDS-2 + BDS-3 and GPS + BDS over 24 h at the WHU2 station.

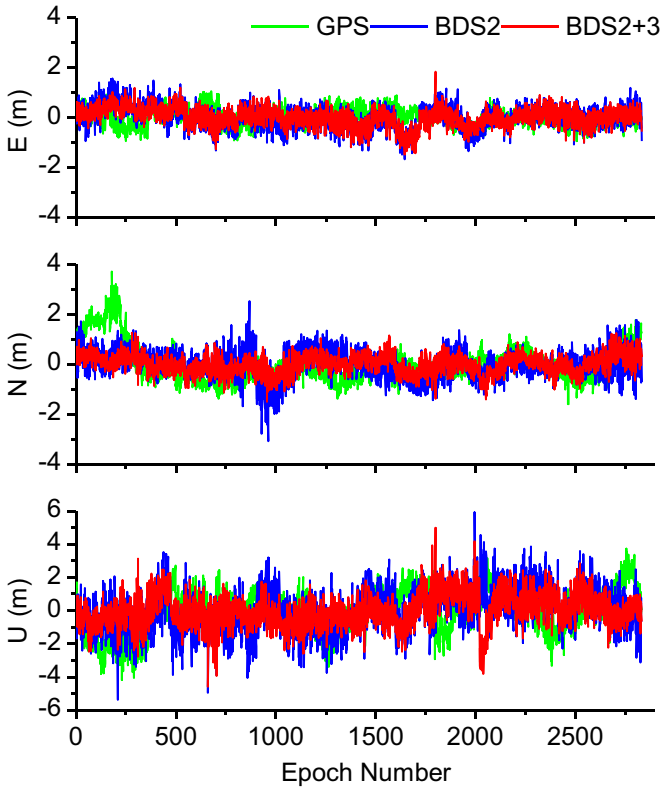

Figure 8. Comparison of E, N, and U standard point positioning residuals by using GPS only, BDS-2 only, and BDS-2 + BDS-3.

only. When BDS-3 observations are added to BDS-2 observations, the RMS values for BDS are 0.376, 0.385, and 0.982 m and the precision is 0.549, 0.641 and 1.422 m. The positioning accuracy and precision obtained for only BDS-2 are lower than that for GPS. However, when the BDS-3 observations are added, the positioning accuracy and precision are significantly improved, which is similar to the conclusions of the previous section.

3.3. Effect of different stochastic models on positioning accuracy

Five different ways are used to reveal the influence of different classification methods and different stochastic models on positioning accuracy. Table 4 shows that if we only use GPS data, the accuracy in the E and U directions is higher than that from BDS-2, and the N direction is slightly lower than that from BDS-2. When BDS observations are simply divided into two types of observations (BDS-2 and BDS-3) the accuracy in all three directions obtained by LS-VCE is slightly poorer compared with those from EDM. When BDS/GPS dual system is employed, the addition of BDS-3 observations can improve positioning accuracy. Compared with the EDM, the accuracy obtained by LS-VCE is improved by almost 15% in the N direction. However, the accuracy improvement is limited in the other two directions or even slightly decreased.

Therefore, we can conclude that the addition of BDS-3 observations can improve the geometric spatial distribution structure of satellites and improve the value of PDOP. Positioning accuracy is also significantly improved, whether using the single BDS or dual system positioning. However, if BDS-3 is simply used as a type of observation for the VCE, because of the current limited number of BDS-3 satellites (as can be seen from figure 2), the positioning results will not be improved.

Even though LS-VCE is a general form of VCE method, it still needs data redundancy. Otherwise, the diagonal elements of the variance-covariance matrix may have negative values, which is unreasonable [46]. Moreover, the corresponding number of loops is also higher. As shown in figure 9, the minimum number of loops in the LS-VCE is two, and the average number of loops is six. There are 24 epochs whose loop numbers are more than 30, which means that the variance computed by LS-VCE may not be as stable as others, and thus affects the accuracy and reliability of the positioning results. It should be pointed out that, if the classification of the observations is incorrect, for example, if the number of observations in one group is significantly higher than that in the other, or there are gross errors in the observations, we cannot get a convergent result using the LS-VCE method. In this case, these epochs are skipped directly in data processing; otherwise, the positioning results will have a large deviation.

4. Improved stochastic model based on LS-VCE

Using a simple method to process a matrix that does not converge or has a negative value in a VCE is a key issue in the estimation process. Because the VCE requires data redundancy to get a reliable positioning result for dynamic single epoch SPP, observations of several epochs were used to form an observation matrix to estimate the variance component. The SPP multiple epoch stochastic model can be given as

$$Q_{L,m} = \sum_{i=1}^{p} \sigma_k \sum_{k=1}^{m} Q_{Lk} \tag{14}$$

where m is the number of epochs. If we divide the entire set of observations into p groups, the unknown variance-covariance

Table 4. RMS values at the WHU2 station using different stochastic models (in meters).

	EDM			LS-VCE		
Constellation	E	N	U	E	N	U
GPS	0.3260	0.7367	1.2486	—	—	—
BDS-2	0.4639	0.5616	1.2919	—	—	—
BDS-2 + 3	0.3757	0.3852	0.9816	0.3872	0.4360	1.010
GPS + BDS-2	0.3088	0.5107	1.1147	0.3261	0.4547	1.0544
GPS + BDS	0.2726	0.4057	0.8977	0.2848	0.3440	0.8331

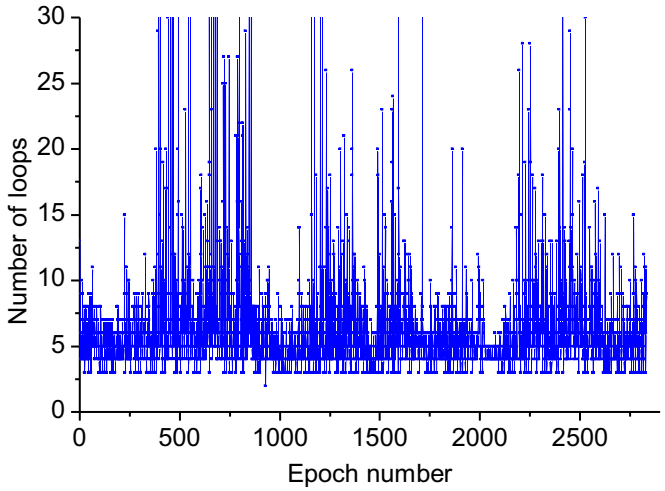

Figure 9. Number of loops in which BDS-2 and BDS-3 are divided into two types of observations using LS-VCE.

components can be separately estimated for each group. The final estimates are then obtained by averaging the groupwise estimates over all p groups as [47]

$$\hat{\sigma}_k = \sum_{i=1}^{p} \hat{\sigma}_{k(i)}/r \tag{15}$$

where $k = 1, 2, \ldots, p$ and $\hat{\sigma}_{k(i)}$ is the kth (co)variance component of the ith group.

We need to be aware of the fact that the dimensions of the observation matrix will be too large if too many epochs are involved in the calculation. For example, when only BDS-2 + 3 observations from ten epochs are used, the dimension of the matrix will reach 151. Therefore, to reduce the computational burden, in the experiment, up to one hour (120 epochs) of data is selected for the VCE and we did not show the specific values of the covariance matrix in the iterative calculation. At the same time, the relationship between the satellite elevation angle and the precision of the observation, which had been discussed by Hu *et al* [42], was also considered in the experiment. In other words, the EDM was used as the original stochastic model. As shown in table 5, three experimental schemes were utilized to estimate the variance components. As mentioned above, external conditions such as the number of satellites, elevation angle, and geometric distribution will influence the precision of different types of

Table 5. Variance component ratio of different types of observations calculated by LS-VCE.

Epoch	BDS-2:BDS-3	GEO:IGOS:MEO	BDS-2:BDS-3:GPS
10	1:2.52	1:2.04:1.94	1:2.20:2.02
30	1:2.02	1:1.87:1.78	1:1.97:1.93
60	1:2.20	1:1.80:1.72	1:1.85:1.83
100	1:1.86	1:1.70:1.53	1:1.74:1.80
120	1:1.71	1:1.61:1.48	1:1.55:1.71

observations. Therefore, to ensure the reliability of the results, we selected data from a whole day rather than a specific time period in the experiment, and we averaged the estimation results as the variance component ratio of different types of observations.

Table 5 shows that there are some differences among the variance ratios of different types of observations calculated by different numbers of observations. It seems that the more observations that were used, the smaller the variance ratio between different types of observations became. In other words, the stochastic model is more important in single epoch SPP. Moreover, according to the results of VCE, we can also see that the variance component ratios of BDS-3 and GPS are very similar, being twice that of BDS-2. Therefore, a new three-step stochastic model is proposed as outlined in the following.

First, a modified EDM model is proposed based on the previously estimated results. The model can be expressed as

$$\delta^2(E) = \begin{cases} \dfrac{\sigma_0^2}{c_t \cdot \sin(E)} & E < 60^\circ \\ \sigma_0^2/c_t & E \geqslant 60^\circ \end{cases}, \tag{16}$$

where c_t is a coefficient for the different types of satellites. For example, if the observations are divided into BDS-2, BDS-3, and GPS or GEO, IGSO and MEO, the coefficient, which can be obtained from table 5, would be 1:2:2. If there are only BDS observations and these are divided into BDS-2 and BDS-3, the coefficients could be 1:2.

Second, we estimate the variance components for each measurement type using LS-VCE. If the LS-VCE cannot converge in the calculation or the matrix elements have negative values, the non-negative least-squares VCE (NNLS-VCE) should be adopted. The variances should be subject to the non-negativity constraints $\sigma \geqslant 0$ to ensure that they are not negative [41]:

Table 6. Average RMS and precision values with different stochastic models (in meters).

	Residual RMS		Precision	
Component	Modified EDM	Improved model	Modified EDM	Improved model
E	0.4672	0.3733	0.4161	0.3516
N	0.5336	0.4979	0.4689	0.3879
U	1.2011	1.0442	1.0363	0.8785

$$\arg\min_{\sigma\geqslant 0} F(\sigma) = \arg\min_{\sigma\geqslant 0}\left(\frac{1}{2}\sigma^T N\sigma - l\sigma\right)$$

where N is given in equation (7) and l is given in equation (8). We used equation (16) as an active set to solve the negative problem, which means that if the unconstrained estimated least-squares coefficient is not positive, then the modified EDM will be used.

Then, we determine the scale factor to update the final weight matrix and calculate the position using least-square equations. In fact, we can also directly use modified EDM. Table 6 shows the precision and RMS values from 46 sites obtained by using the modified EDM and the proposed model. We see that, the precision of the three directions of E, N and U using modified EDM has been improved from 0.529, 0.586, and 1.321 to 0.416, 0.469, and 1.036 m, respectively, compared with that of EDM. The precision of the improved LS-VCE model has been improved to 0.352, 0.388, and 0.879 m, respectively. Even though the modified EDM can improve positioning precision, the RMS values improvement is not obvious. The proposed model demonstrates significant improvement in precision and accuracy in the three directions of E, N, and U, especially in the E direction, in which accuracy has increased from 0.502 to 0.373 m. The accuracy in the N direction increased from 0.533 to 0.498 m, and that in the U direction increased from 1.333 to 1.044 m.

If some epochs are not available or the convergence time is too long, as mentioned above, this will have a great adverse effect on navigation users. Therefore, in practical applications, it must be ensured that, in the absence of gross errors, all epochs can obtain more accurate positioning results in a short time. The unstable numbers of daily observations are shown in figure 9 using blue solid points. Because not all stations can receive BDS-2 observations, the number of unstable epochs, that is, the number of epochs skipped can reach up to 705. With the improved stochastic model, a stable solution can be obtained for all epochs. In addition, comparing tables 3 and 6, we can see that positioning accuracy is also slightly increased after the improved stochastic model is adopted.

Moreover, the times taken to calculate daily observations using the elevation angle model and the improved model are also shown in figure 10. Because the LS-VCE method requires an iterative operation, the calculation time is longer than that of the EDM. However, only one of the 46 sites had a significant increase in computing time, which was 142 s. The average increase in time was 28 s, which means that each epoch calculation time only increased by 0.01 s. Therefore, we can conclude that the improved stochastic model can increase positioning accuracy and ensure that a reliable solution can be obtained for each epoch, while not significantly increasing the computational burden on the computer.

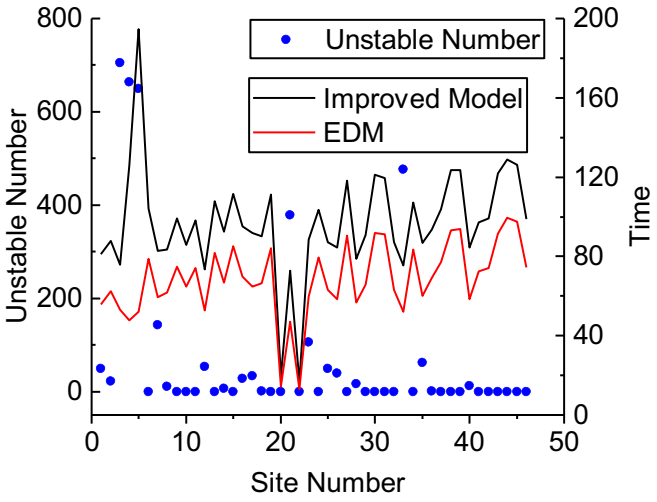

Figure 10. Time cost of a daily observation computation and the number of unstable epochs using the improved method. The left axis represents the number of unstable results at one site using the traditional LS-VCE, and the right axis represents the time it takes for a single-epoch SPP of 1 d.

5. Conclusions

This study focused on BDS and GPS stochastic model estimation in multi-GNSS SPP processing based on GPS L1 and BDS B1 code observations. We first assessed the contribution of BDS-3 to multi-GNSS SPP using 46 globally distributed stations. Our results demonstrated that, with the additional of BDS-3 observations, the number of visible satellites increased significantly, especially for the Western Hemisphere. However, positioning accuracy will not be significantly improved, and it can become even poorer if the stochastic model is not appropriate. For a single site, the addition of BDS-3 observations offers a significant improvement in the number of visible satellites, PDOP values and positioning accuracy.

Furthermore, a comprehensive stochastic model for multi-GNSS positioning is proposed based on LS-VCE. We used multiple epochs to estimate the variance component ratio of different types of observations. Our estimates showed that the fewer the number of epochs employed, the more important became the stochastic model. A modified EDM and improved LS-VCE stochastic model are proposed with the help of variance component ratios. Based on the obtained results, the accuracy of E, N U and U directions are 0.373, 0.498 and 1.044 m in comparison to EDM method with 0.502, 0.533 and 1.333 m, respectively. In addition, the precision of the three directions is improved from 0.529, 0.604, and 1.312 m to 0.352, 0.388 and 0.879 m, respectively. The experimental results indicate that the improved LS-VCE stochastic model can significantly improve multi-GNSS SPP precision and accuracy compared with the modified EDM, while not significantly

increasing calculation time. Moreover, with the application of the improved LS-VCE model, reliable results can be obtained for all epochs.

Acknowledgments

This work is sponsored by the National Natural Science Foundation of China (Grant Nos. 41704036 and 41904027) and a project funded by the NASG Key Laboratory of Land Environment and Disaster Monitoring (Grant No. LEDM2014B02). The authors would like to thank the IGS MGEX for providing multi-GNSS ground tracking data.

ORCID iDs

Hong Hu https://orcid.org/0000-0002-7810-1528
Feng Zhou https://orcid.org/0000-0002-0183-7940

References

[1] Parvazi K, Farzaneh S and Safari A 2020 Role of the RLS-VCE-estimated stochastic model for improvement of accuracy and convergence time in multi-GNSS precise point positioning *Measurement* **165** 108073
[2] Koch K R 1999 *Parameter Estimation and Hypothesis Testing in Linear Models* 2nd edn (Berlin: Springer)
[3] Li B, Shen Y and Lou L 2011 Efficient estimation of variance and covariance components: a case study for GPS stochastic model evaluation *IEEE Trans. Geosci. Remote Sens.* **49** 203–10
[4] Teunissen P J G 2006 *Testing Theory: An Introduction* 2nd edn (Delft: Delft University Press)
[5] Baarda W 1968 *A Testing Procedure for Use in Geodetic Networks* (Delft: Rijkscommissie voor Geodesie)
[6] Li B, Lou L and Shen Y 2016 GNSS elevation-dependent stochastic modeling and its impacts on the statistic testing *J. Surv. Eng.* **142** 04015012
[7] Jin X and de Jong C D 1996 Relationship between satellite elevation and precision of GPS code observations *J. Navig.* **49** 253–65
[8] Wanninger L and Beer S 2015 BeiDou satellite-induced code pseudorange variations: diagnosis and therapy *GPS Solut.* **19** 639–48
[9] Takasu T and Yasuda A 2009 Development of the low-cost RTK-GPS receiver with an open source program package RTKLIB *12th IAIN World Congress Int. Symp. on GPS/GNSS* (http://gpspp.sakura.ne.jp/paper2005/isgps_2009_rtklib_revA.pdf)
[10] Herring T A, King R W and McClusky S C 2010 *GAMIT Reference Manual* (USA: MIT)
[11] Dach R, Lutz S, Walser P and Fridez P 2015 *Bernese GNSS Software Version 5.2* (University of Bern)
[12] Tiberius C and Kenselaar F 2003 Variance component estimation and precise GPS positioning: case study *J. Surv. Eng.* **129** 11–18
[13] Amiri-Simkooei A R, Teunissen P J G and Tiberius C C J M 2009 Application of least-squares variance component estimation to GPS observables *J. Surv. Eng.* **35** 149–60
[14] Bona P 2000 Precision, cross correlation, and time correlation of GPS phase and code observations *GPS Solut.* **4** 3–13
[15] Brunner F K, Hartinger H and Troyer L 1999 GPS signal diffraction modelling: the stochastic SIGMA-δ model *J. Geod.* **73** 259–67
[16] Hartinger H and Brunner F K 1999 Variances of GPS phase observations: the SIGMA-ε model *GPS Solut.* **2** 35–43
[17] Aquino M, Monico J, Dodson A, Marques H, De Franceschi G, Alfonsi L, Romano V and Andreotti M 2009 Improving the GNSS positioning stochastic model in the presence of ionospheric scintillation *J. Geod.* **83** 953–66
[18] Silva H A, Camargo P O, Monico J F G, Aquino M, Marques H A, De Franceschi G and Dodson A 2010 Stochastic modelling considering ionospheric scintillation effects on GNSS relative and point positioning *Adv. Space Res.* **45** 1113–21
[19] Li B 2016 Stochastic modeling of triple-frequency BeiDou signals: estimation, assessment and impact analysis *J. Geod.* **90** 593–610
[20] Li B, Zhang L and Verhagen S 2017 Impacts of BeiDou stochastic model on reliability: overall test, w-test and minimal detectable bias *GPS Solut.* **21** 1095–112
[21] CSNO 2017 *BeiDou Navigation Satellite System Signal in Space Interface Control Document B1C and B2a Open Service Signal (Test Version)* (Beijing: China Satellite Navigation Office)
[22] Zhao Q, Wang C, Guo J, Wang B and Liu J N 2018 Precise orbit and clock determination for BeiDou-3 experimental satellites with yaw attitude analysis *GPS Solut.* **22** 4
[23] CSNO 2018 *Development of the BeiDou Navigation Satellite System* (Beijing: China Satellite Navigation Office)
[24] Qu L, Du M, Wang J, Gao Y, Zhao Q, Zhang Q and Guo X 2019 Precise point positioning ambiguity resolution by integrating BDS-3e into BDS-2 and GPS *GPS Solut.* **23** 63
[25] Su K and Jin S 2019 Triple-frequency carrier phase precise time and frequency transfer models for BDS-3 *GPS Solut.* **23** 86
[26] Shi J, Ouyang C Y, Huang Y H and Peng W J 2020 Assessment of BDS-3 global positioning service: ephemeris, SPP, PPP, RTK, and new signal *GPS Solut.* **24** 81
[27] Brack A 2017 Reliable GPS + BDS RTK positioning with partial ambiguity resolution *GPS Solut.* **24** 1093–1093
[28] Zhao S H, Cui X W and Lu M Q 2019 Single point positioning using full and fractional pseudorange measurements from GPS and BDS *Surv. Rev.* (accepted) (available at: www.tandfonline.com/doi/full/10.1080/00396265.2019.1683327)
[29] Zhang B, Hou P, Liu T and Yuan Y 2020 A single-receiver geometry-free approach to stochastic modeling of multi-frequency GNSS observables *J. Geod.* **94** 37
[30] Miao W, Li B, Zhang Z and Zhao X 2020 Combined BeiDou-2 and BeiDou-3 instantaneous RTK positioning: stochastic modeling and positioning performance assessment *J. Spat. Sci.* **65** 7–24
[31] Klobuchar J A 1987 Ionospheric time-delay algorithms for single-frequency GPS users *IEEE Trans. Aerosp. Elecron. Syst.* **23** 325–31
[32] Saastamoinen J 1973 Contributions to the theory of atmospheric refraction *Bull. Géodésique* **107** 13–34
[33] Teunissen P J G and Amiri-Simkooei A R 2008 Least-squares variance component estimation *J. Geod.* **82** 65–82
[34] Teunissen P J G and Montenbruck O 2017 *Springer Handbook of Global Navigation Satellite Systems* (Berlin: Springer)
[35] Helmert F R 1907 *Die Ausgleichungsrechnung nach der Methode der Kleinsten Quadrate* Zweite edn (Leipzig: Teubner)
[36] Koch K R 1978 Schätzung von Varianzkomponenten *Allg. Vermess.-Nachr.* **85** 264–9
[37] Rao C R 1971 Estimation of variance and covariance components—MINQUE theory *J. Multivariate Anal.* **1** 257–75
[38] Koch K R 1986 Maximum likelihood estimate of variance components *Bull. Gæodésique* **60** 329–38
[39] Teunissen P J G 2004 Towards a least-squares framework for adjusting and testing of both functional and stochastic

models (*Mathematical Geodesy and Positioning Series 26*) (Delft: Geodetic Computing Centre) (available at: https://gnss.curtin.edu.au/wp-content/uploads/sites/21/2016/04/Teunissen2004Towards.pdf)

[40] Amiri-Simkooei A R 2007 Least-squares variance component estimation: theory and GPS applications PhD Thesis Delft University of Technology, Delft, The Netherlands

[41] Amiri-Simkooei A R 2016 Non-negative least-squares variance component estimation with application to GPS time series *J. Geod.* **90** 451–66

[42] Hu H, Jin S G, Kang R H and Cao X Y 2018 BeiDou code pseudorange precision estimation and time correlation analysis from trimble Net-R9 and ComNav 708 receivers *Remote Sens.* **10** 1083

[43] Guo F, Zhang X, Wang J and Ren X 2016 Modeling and assessment of triple-frequency BDS precise point positioning *J. Geod.* **90** 1223–35

[44] CSNO 2019 *BeiDou Navigation Satellite System Signal in Space Interface Control Document Open Service Signal B1I (Version 3.0)* (Beijing: China Satellite Navigation Office)

[45] Xu G 2007 *GPS: Theory, Algorithms and Applications* 2nd edn (Berlin: Springer)

[46] Cai C S, Pan L and Gao Y 2014 A precise weighting approach with application to combined L1/B1 GPS/BeiDou positioning *J. Navig.* **67** 911–25

[47] Amiri-Simkooei A R, Jazaeri S, Zangeneh-Nejad F and Asgari J 2016 Role of stochastic model on GPS integer ambiguity resolution success rate *GPS Solut.* **20** 51–61